Close encounters of the protostellar kind in IC 1396N

M. T. Beltrán, F. Massi, F. Fontani, C. Codella, R. López

A&A 542, L26 (2012)
DOI: 10.1051/0004-6361/201219166

Astronomy & Astrophysics

Letter to the Editor

Close encounters of the protostellar kind in IC 1396N⋆

M. T. Beltrán[1], F. Massi[1], F. Fontani[1], C. Codella[1,2], and R. López[3]

[1] INAF – Osservatorio Astrofisico di Arcetri, Largo E. Fermi 5, 50125 Firenze, Italy
e-mail: mbeltran@arcetri.astro.it
[2] UJF-Grenoble 1/CNRS-INSU, Institut de Planétologie et d'Astrophysique de Grenoble (IPAG) UMR 5274, Grenoble, France
[3] Departament d'Astronomia i Meteorologia, Universitat de Barcelona, Martí i Franquès 1, 08028 Barcelona, Catalunya, Spain

Received 5 March 2012 / Accepted 9 May 2012

ABSTRACT

We have mapped in the 2.7 mm continuum and ^{12}CO with the PdBI the IR-dark "tail" that crosses the IC 1396N globule from south to north, and is the most extincted part of this cloud. These observations have allowed us to distinguish all possible associations of molecular hydrogen emission features by revealing two well-collimated low-mass protostellar outflows at the northern part of the globule. The outflows are located almost in the plane of the sky and are colliding with each other towards the position of a strong 2.12 μm H_2 line emission feature.

Key words. ISM: individual objects: IC 1396N – ISM: jets and outflows – stars: formation – infrared: ISM

1. Introduction

IC 1396N is a bright-rimmed cloud (BRC38; Sugitani et al. 1991), located at a distance of 750 pc (Matthews 1979), which has been extensively studied by our group (Nisini et al. 2001; Codella et al. 2001; Beltrán et al. 2002, 2004, 2009; Fuente et al. 2009). The cloud shows a cometary structure elongated in the south-north direction, with the globule head located at the south, facing the O6.5 exciting star HD 206267, and the tail pointing to the north. Towards the globule head, one finds the intermediate-mass protostar IRAS 21391+5802 (BIMA 2), which is associated with multiple millimeter compact sources and powers a molecular outflow (Codella et al. 2001; Beltrán et al. 2002; Neri et al. 2007; Fuente et al. 2009). Near-infrared (NIR) images have revealed a number of small-scale 2.12 μm H_2 line emission features and Herbig-Haro (HH) flows spread all over the globule (Nisini et al. 2001; Sugitani et al. 2002; Reipurth et al. 2003; Caratti o Garatti 2006; Beltrán et al. 2009), as well as an IR-dark "tail" that crosses the cloud from south to north and is clearly pinpointed in the *JHK′* composite image (see Fig. 1 of Beltrán et al. 2009 and Fig. 1a). This IR-dark "tail" is well-traced in both CO and high-density tracers such as CS and $H^{13}CO^+$ (Codella et al. 2001; Sugitani et al. 2002).

Deep sub-arcsecond 2.12 μm H_2 1–0 S(1) line emission observations carried out with the TNG telescope (Beltrán et al. 2009) resolved the emission features spread throughout the region into several chains of knots. In a few cases, these strands of H_2 knots have a jet-like morphology, which suggests that they could trace different flows (Nisini et al. 2001; Beltrán et al. 2009). Towards the northern part of the globule, Nisini et al. (2001) proposed that some of these knots could be associated with the CO molecular outflow discovered by Codella et al. (2001), and Beltrán et al. (2009) suggested that strand of knots located at both sides of the IR-dark "tail" could be associated with each other and be part of long flows with lengths ranging from 0.18 to more than 0.4 pc, and that the powering sources were embedded in the "tail".

To test the hypothesis that some of the molecular hydrogen emission features could be associated with long flows crossing the northern part of IC 1396N, we mapped with the IRAM Plateau de Bure Interferometer (PdBI) the whole IR-dark "tail" in ^{12}CO, which is the most sensitive outflow tracer and should help us to trace the cold-warm flow component that is overlooked by the hotter component tracer H_2. The "tail" was also mapped in the continuum at 2.7 mm to search for the possible outflow powering sources that according to Beltrán et al. (2009) should be hidden there. In this letter, we present the first results of this study, which confirm the scenarios proposed by Beltrán et al. (2009), including the collision of two of these flows.

2. Observations

We carried out seven-point mosaic observations of the IR-dark "tail" in IC 1396N in the 2.7 mm continuum and ^{12}CO (1–0) line emission with the PdBI on 2010 July 24 and 27, and November 4, in the D and C configurations. The inner hole in the (u, v)-plane has a radius of 7 kλ. Line data were smoothed to a spectral resolution of 1 km s^{-1}. The maps were created with natural weighting, attaining a resolution of 2.″9 × 2.″8, but to highlight the continuum and line emission, the final maps were reconstructed with a circular synthesized beam of 4″ × 4″. The 1σ noise is 0.25 mJy beam^{-1} for the continuum map and 10 mJy beam^{-1} channel^{-1} for the CO line map.

3. Analysis and discussion

3.1. The embedded protostars

The continuum observations of the northern part of the IR-dark "tail" detected two embedded cores, which we call sources I and C, powering well-collimated outflows (with collimation factors >5 towards the central part of the outflows; Fig. 1b) and separated by ∼0.1 pc. The source C was first detected at 1.25 mm with the IRAM 30-m telescope by Codella et al. (2001), who

⋆ Based on observations carried out with the IRAM Plateau de Bure. IRAM is supported by INSU/CNRS (France), MPG (Germany), and IGN (Spain).

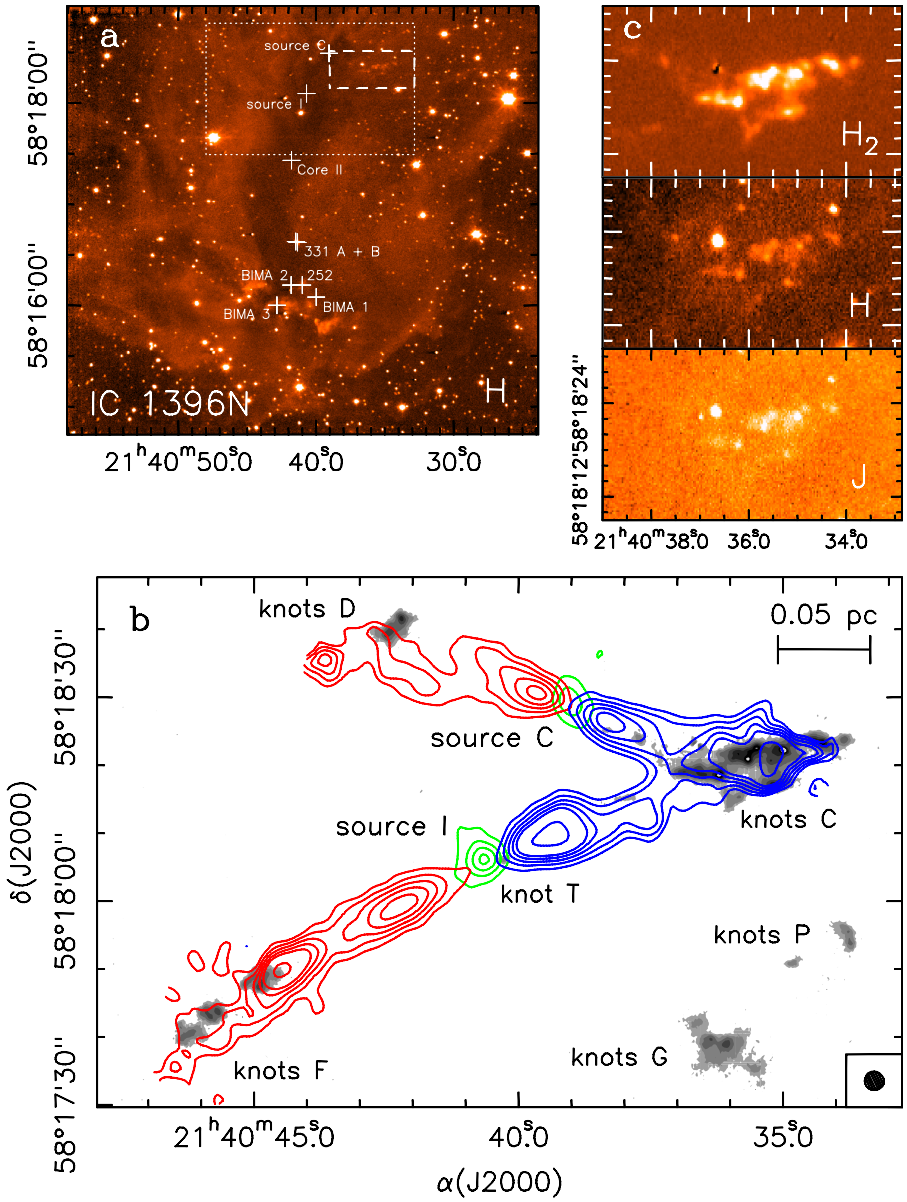

Fig. 1. **a)** *H*-band image of IC 1396N taken with NICS at TNG. The white crosses show the positions of the 3.1 mm sources, BIMA 1, 2, and 3 from Beltrán et al. (2002), the Class I sources # 252 and # 331 (binary, A+B) (Beltrán et al. 2009), the two embedded sources I and C, which are powering the outflows in panel b (Codella et al. 2001; this paper), and core II (Sugitani et al. 2002). The dotted and dashed boxes indicate the region mapped in panels b and c, respectively. **b)** H_2 (2.12 μm) image (continuum-subtracted) in grey-scale (Beltrán et al. 2009), 2.7 mm continuum emission in green contours and ^{12}CO (1–0) emission averaged over the [±8, ±38] km s^{-1} velocity interval in red and blue contours towards the northern part of the IC 1396N cloud. Contour levels are 3, 6, 9, 12, 15, and 24 times 1σ, where 1σ is 0.25 mJy beam^{-1} for the continuum, and 4 mJy beam^{-1} for the CO emission. The PdBI synthesized beam is shown in the lower right corner. **c)** H_2 (continuum-subtracted) (*top*), *H*-band (*middle*), and *J*-band (*bottom*) image towards the chain of knots C (Beltrán et al. 2009).

suggested that it was the powering source of the northern bipolar outflow mapped in ^{12}CO (2–1) with an angular resolution of 10″. However, this is the first time that the source is mapped and at high angular resolution. The existence of source I and the bipolar outflow that is driving had been suggested by Beltrán et al. (2009) (see next section), and our observations here confirm this idea. This new source could be associated with the $H^{13}CO^+$ peak labeled as core I by Sugitani et al. (2002). The mass of the sources was estimated assuming a dust opacity of 1.15 cm^2 g^{-1} at 115 GHz (Beckwith et al. 1990) and a gas-to-dust ratio of 100. Since the dust temperature, $T_{\rm dust}$, of the sources is unknown, we estimated the masses for 10 K and 20 K, which are the typical temperatures of the gaseous envelopes of low-mass protostars. The mass of source I is ~0.5 $M_\odot$ (for $T_{\rm dust}$ = 10 K) and ~0.2 $M_\odot$ (for $T_{\rm dust}$ = 20 K), and that of source C is ~0.3 $M_\odot$ (for $T_{\rm dust}$ = 10 K) and ~0.1 $M_\odot$ (for $T_{\rm dust}$ = 20 K).

3.2. The colliding molecular outflows

The elongated structure and the very well-defined bipolar morphology of the two molecular outflows mapped in ^{12}CO (1–0) (Fig. 1b), suggest that they are close to the plane of the sky. Both outflows are associated with 2.12 μm H_2 emission. The blueshifted lobes of the two bipolar outflows strongly overlap towards the position of the H_2 strand of knots C. The northern outflow, named N, is being powered by source C and is oriented in the northeast-southwest direction. Nisini et al. (2001) and Beltrán et al. (2009) suggested that it could be associated with the strand of H_2 knots D and C. As seen in Fig. 1b, the CO emission indeed complements the H_2 emission where the excitation conditions and the opacity of the material are different. On the other hand, the southern outflow, named S, which is driven by source I and oriented in the southeast-northwest direction, had never been mapped before. Beltrán et al. (2009) had proposed that the chains of H_2 knots F, T, and C could be associated with and be part of the same flow, which would have a length of ~0.4 pc, as the CO observations have confirmed. These authors had also predicted that the driving source, in this case source I, should be embedded in the dense gas mapped in CS by Codella et al. (2001) and in $H^{13}CO^+$ (core I) by Sugitani et al. (2002). According to the correlations between driving source and outflow properties of Cabrit & Bertout (1992), the bolometric luminosity of the powering sources should be <10 $L_\odot$. The

Table 1. Properties of the molecular outflows[a].

Outflow	$R \cos i$ (pc)	$t_{out} \cot i$ (yr)	T_{ex} (K)	M_{out} ($M_\odot$)	$\dot{M}_{out} \tan i$ ($M_\odot$ yr^{-1})	$P \sin i$ ($M_\odot$ km s^{-1})	$E \sin^2 i$ (10^{43} erg)	$F \sin^2 i/\cos i$ ($M_\odot$ km s^{-1} yr^{-1})	$L_{mech} \sin^3 i/\cos i$ ($L_\odot$)
N Blue	0.13	3.5×10^3	10	3.5×10^{-3}	1.0×10^{-6}	0.06	1.2	1.7×10^{-5}	0.03
N Red	0.14	3.6×10^3	10	2.9×10^{-3}	0.8×10^{-6}	0.05	0.9	1.4×10^{-5}	0.02
N Total	0.27	3.6×10^3	10	6.4×10^{-3}	1.8×10^{-6}	0.11	2.1	3.1×10^{-5}	0.05
S Blue	0.19	4.8×10^3	10	5.8×10^{-3}	1.2×10^{-6}	0.09	1.7	1.9×10^{-5}	0.03
S Red	0.19	4.8×10^3	10	5.4×10^{-3}	1.1×10^{-6}	0.10	2.2	2.1×10^{-5}	0.04
S Total	0.38	4.8×10^3	10	11.2×10^{-3}	2.3×10^{-6}	0.19	3.9	4.0×10^{-5}	0.07

Notes. [(a)] Estimated values. The outflow parameters should be corrected if the inclination angle with respect to the plane of the sky, i, is known. Blueshifted emission averaged over the velocity range [−38, −8] km s^{-1} and redshifted one over [+8, +38] km s^{-1}. Momenta and kinetic energies are calculated relative to the cloud velocity, $V_{LSR} = 0$ km s^{-1}.

parameters of the outflows, which are estimated assuming that the CO emission in the wings is in local thermal equilibrium and optically thin, are given in Table 1. The outflow parameters and the masses of the driving sources are consistent with those of low-mass protostars (e.g., Arce et al. 2007, and references therein). Since the CO spectra exhibit prominent self-absorption at the cloud velocity and it is impossible to derive the excitation temperature, T_{ex}, from the brightness temperature, the outflow parameters were estimated assuming $T_{ex} = 10$ K, which was the value adopted by Codella et al. (2001) for the northern outflow. We used an [H_2]/[CO] abundance ratio of 10^4 (e.g. Scoville et al. 1986). To calculate the parameters of the blueshifted lobes, we assumed that half of the CO emission seen towards the feature C is associated with outflow N and half with outflow S. That the parameters of the redshifted lobes are similar to those of the blueshifted lobes for both outflows suggests that this assumption is correct. The parameters need to be corrected by the factors indicated in Table 1 if the inclination angle of the flow with respect to the plane of the sky, i, is known. On the basis of the morphology of the outflows, $i \lesssim 10°$.

In the scenario proposed by Beltrán et al. (2009), the outflows N and S would collide towards the position of the chain of knots C and this would explain the strong H_2 emission observed towards this feature. As previously mentioned, the blueshifted lobes of the CO bipolar outflows do indeed overlap towards the position of the strand of knots C (Fig. 1b). However, the collision of outflows is not the only possible explanation of this morphology. The overlapping of the blueshifted emission might also indicate that the outflows are colliding with the same dense clump, or are merely a projection effect. In the latter scenario, the outflows would be in different planes of the sky and would be shocking with different dense clumps aligned along the line of sight. However, that the outflows are almost in the same plane (that of the sky), that the powering sources are at the same systemic velocity, $V_{LSR} \sim 0$ km s^{-1}, and that some observational facts favor a collision (see next), either with the same clump or between outflows, rules out a chance superposition of the outflows.

Figure 2 shows the position-velocity (PV) plots along the major axis of the outflows. The cuts were made along PA = −102° for outflow N and PA = −24° for outflow S, and all the plots were obtained after averaging the emission along the direction perpendicular to the cut for the purpose of increasing the S/N of the plots. The clumpy morphology of the outflows (Figs. 1b and 2) could be the result of episodic mass-loss events. As seen in Fig. 2, the velocity of the CO emission increases rapidly with increasing distance from the powering sources. This is clearly visible for the southern outflow. The material accelerates until it reaches the position of the H_2 knots: the strand of knots D and F, located at the end of the redshifted lobes of the N and S outflows, respectively, and the group of knots C, at the end of the blueshifted lobes. At the position of the H_2 knots, there is an increase in the extreme emission velocity ($V \gtrsim 40$ km s^{-1}) for the lowest emission contour level, while the bulk of the emission abruptly decelerates and has a much lower velocity ($V \simeq 10$–20 km s^{-1}). This is less evident for the knots D, which reach velocities of only ∼20 km s^{-1}, although this could be due to the lower sensitivity at the edge of the map to higher velocities. For the chain of knots C, the bulk of the emission clearly delineates an inverse triangle shape for both outflows, with the velocity of the material slowly increasing from the position of knot C5 (the first knot of the main H_2 emission feature encountered by the blue lobes) to the position where the material at the lowest emission level reaches the maximum velocity, and then decelerating up to the position of knot C16 (the last knot of the main H_2 emission feature encountered by the blue lobes). The morphology of the CO emission could be explained in terms of outflowing material that is impacting, either with a dense clump or with another outflow, at the position of the H_2 knots, giving rise to the NIR emission.

The H_2 emission of the group of knots C is the strongest of the entire northern part of the globule. The integrated line emission of this feature, summing the emission of all the individual knots, is 485.4×10^{-15} mW m^{-2} (Beltrán et al. 2009). This value is much higher than the integrated molecular hydrogen emission of the strand of knots D (52.8×10^{-15} mW m^{-2}) and F (92.9×10^{-15} mW m^{-2}). This clear asymmetry at both ends of the outflows, in terms of both morphology and intensity of the feature, led us to think that the shock that is taking place at the position of the knots C is exceptional. The knots D, F, and C are also visible at 4.5 μm (see Fig. 5 of Beltrán et al. 2009), in which case, the feature C is also the strongest. We investigated whether this could be due to extinction. Assuming that knots D and F have the same integrated emission as knots C but are more extincted, to reproduce the same integrated fluxes, the visual extinction, A_V, should be ∼21 mag higher in D than in C, and ∼16 mag higher in F than in C. From the color–magnitude of Beltrán et al. (2009), and from estimates based on the CO and CS emission data of Codella et al. (2001), the maximum extinction through the northern end of the globule "tail" is $A_V < 20$ mag. Although we cannot exclude that the extinction is severely affecting the intensities of the knots D and F, it seems unlikely that the difference in extinction between molecular hydrogen features located outside the IR-dark "tail", which is the

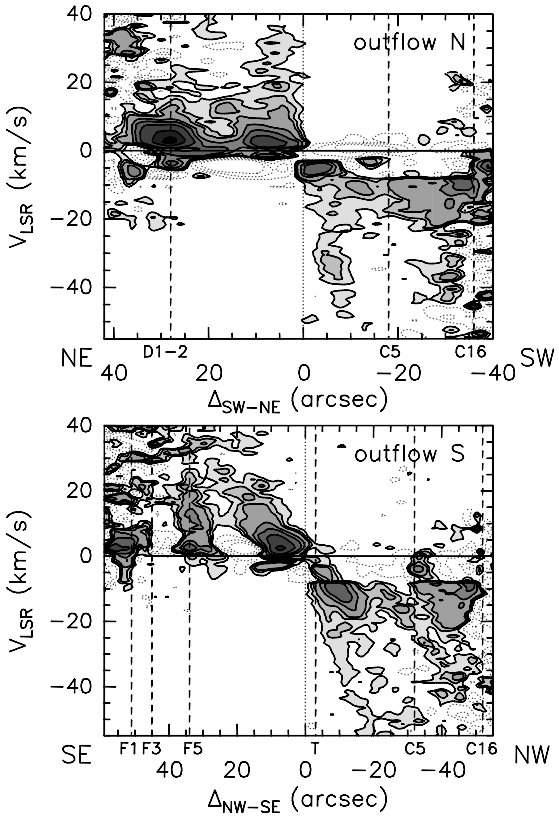

Fig. 2. ^{12}CO (1–0) position-velocity plots along the major axis of the outflows, with PA = −102° for outflow N, and PA = −24° for outflow S. The offsets are measured from the position of source C, α(J2000) = $21^h40^m39\overset{s}{.}04$, δ(J2000) = +58°18′29″.8, for outflow N and of source I, α(J2000) = $21^h40^m40\overset{s}{.}66$, δ(J2000) = +58°18′06″.0, for outflow S, and are positive towards the northeast and southeast, respectively. Contour levels are −12, −9, −3, 3, 6, 9, 12, 27, 45, 90, and 145 times 1σ, where σ is 10 mJy beam^{-1}. The horizontal line indicates the V_{LSR}. The vertical dotted line indicates the position of the powering sources, and the vertical dashed lines the position of the H_2 knots (Beltrán et al. 2009).

most extincted part of the globule, are so large. Spectra taken towards the position of knots F and C (Massi et al., in prep.), show a richness of other H_2 transitions in *J*-, *H*-, and *K*-bands. The emission is much stronger in C than in F, which would explain why the strand of knots C is clearly visible in the *H* and *J*-band images (Fig. 1c).

The CO and H_2 emission clearly indicates that there is a shock at the position of the strand of knots C. To distinguish between the two possible scenarios, that is, that the outflows are colliding with each other or are impacting with the same dense clump, we analyzed the emission at the cloud velocity traced by ^{12}CO in the [−8, +8] km s^{-1} velocity range (the cloud V_{LSR} is ∼0 km s^{-1}). The average CO emission in this velocity interval does not show any compact clump at that position. The negative contours visible in the PV plots at the position of the knots C at systemic velocities would indicate that the interferometer has filtered out only extended emission. A compact dense clump is similarly invisible in the channel maps of the high-density tracer CS (3–2) (Codella et al. 2001). Therefore, the most plausible explanation for the NIR and CO emission is that the outflows are located in the same plane, as already suggested by their well-defined bipolar morphology, and are indeed colliding. This scenario is particularly interesting because the collision would take place in a very pristine environment, where sources C and I would be the only embedded protostars. As seen in Fig. 1a, most of the protostars are located in the southern part of the IR-dark "tail". As far as we know, possible outflow interactions have previously been reported in the crowded L1448 region, where multiple protostars and molecular outflows have been detected (Barsony et al. 1998; Kwon et al. 2006). However, the most likely explanation of those interactions are not outflow collisions but outflow-dense core shocks (Barsony et al. 1998).

Assuming that both outflows are randomly oriented, the probability of such an event is low (∼5%), if one considers the case of two sources separated by a short distance (0.2 pc), powering outflows with 0.01 pc of radius, in which one of the outflows is perpendicular to the line joining the two sources. The probability is higher (∼10−20%) if one considers the case in which the direction of both outflows is allowed to vary. We note that the probability will be even higher if the separation between the sources is smaller or the opening angle of the outflow higher. Therefore, that, to our knowledge, clear cases of outflow collisions have not been found is not because of the rather low probability of such an event but to the practical difficulty in observing two very close sources in a similar evolutionary state located at a distance that allows us to resolve the emission of their respective outflows.

4. Conclusions

We have presented evidence for the collision of the outflows N and S observed in the northern part of the bright-rimmed cloud IC 1396N based on the overlap of the CO blueshifted lobes, the well-defined bipolarity of the outflow, which indicates that both outflows are located close to the plane of the sky, the strong H_2 emission towards the position where the two blueshifted lobes overlap (strand of knots C), and the non-detection of a compact dense clump at the position of the putative shock. Additional high-angular resolution observations of shock tracers, such as SiO, would be needed to confirm this collisional scenario. Observing lower SiO velocities over the blueshifted interacting region than for the redshifted emission of the outflow would further support this scenario. The collision scenario would imply, if confirmed, that the star formation in this globule is aligned along a preferential direction.

Acknowledgements. This work benefited from research funding from the European Community's Seventh Framework Programme.

References

Arce, H. G., Shepherd, D., Gueth, F., et al. 2007, in Protostars and Planets V, ed. B. Reipurth, D. Jewitt, & K. Keil (Tucson: University of Arizona Press), 245
Barsony, M., Ward-Thompson, D., André, P., & O'Linger, J. 1998, ApJ, 509, 733
Beckwith, S. V. W., Sargent, A. I., Chini, R. S., & Guesten, R. 1990, AJ, 99, 924
Beltrán, M. T., Girart, J. M., Estalella, R., et al. 2002, ApJ, 573, 246
Beltrán, M. T., Girart, J. M., Estalella, R., & Ho, P. T. P. 2004, A&A, 426, 941
Beltrán, M. T., Massi, F., López, R., et al. 2009, A&A, 504, 97
Cabrit, S., & Bertout, C. 1992, A&A, 261, 274
Caratti o Garatti, A., Giannini, T., Nisini, B., & Lorenzetti, D. 2006, A&A, 449, 1077
Codella, C., Bachiller, R., Nisini, B., et al. 2001, A&A, 376, 271
Fuente, A., Castro-Carrizo, A., Alonso-Albi, T., et al. 2009, A&A, 507, 1475
Kwon, W., Looney, L. W., Crutcher, R. M., & Kirk, J. M. 2006, ApJ, 653, 1368
Matthews, T. J. 1979, A&A, 75, 345
Neri, R., Fuente, A., Ceccarelli, C., et al. 2007, A&A, 468, L33
Nisini, B., Massi, F., Vitali, F., et al. 2001, A&A, 376, 553
Reipurth, B., Armond, T., Raga, A., & Bally, J. 2003, ApJ, 593, L47
Scoville, N. Z., Sargent, A. I., Sanders, D. B., et al. 1986, ApJ, 303, 416
Sugitani, K., Fukui, Y., & Ogura, K. 1991, ApJS, 77, 59
Sugitani, K., Tamura, M., Nakaya, H., et al. 2002, Proc. the IAU 8th Asian-Pacific Regional Meeting, Vol. II, ed. S. Ikeuchi, J. Hearnshaw, & T. Hanawa (Tokyo: ASJ), 213